Regenerative Reponses of the Subventricular Zone Following Pediatric Traumatic Brain Injury

Matthew T. Goodus, Alanna M. Guzman, Frances Calderon,

Yuhui Jiang and Steven W. Levison

Department of Neurology and Neuroscience, Graduate School of Biomedical Sciences,

Rutgers University, Newark, NJ, USA.

*Address correspondence and reprint requests to:

Steven W. Levison, PhD

Laboratory for Regenerative Neurobiology

Department of Neurology and Neuroscience

New Jersey Medical School, Rutgers University

205 South Orange Avenue

Newark, NJ 07103

PH (973) 972-5162

FAX: 973 972-2668

Email: steve.levison@Rutgers.edu

Key Words: subventricular zone, neurogenesis, stem cells, progenitors, rats, mice

Running Title: NSC expansion after pediatric TBI

Abstract

Pediatric Traumatic Brain Injury (TBI) is a significant problem that affects many children each year. Progress is being made in developing neuroprotective strategies to combat such injuries; however, investigators are a long way from therapies to fully preserve injured neurons and glia. To restore neurological function, regenerative strategies will be required. The Subventricular Zone (SVZ) harbors dividing cells that have the potential to regenerate multiple types of brain cells after injury; therefore, we evaluated regenerative responses of the SVZ after pediatric. We used controlled cortical impact (CCI) injury to produced comparable damage to the somatosensory cortex of rats at postnatal day 6 (P6), P11, P17 and P60 and mice at P14. At both 48 and 96 hours after injury, the mitotic indices of animals injured at pediatric ages were significantly increased vs. sham operated and naïve controls and the regenerative response was more robust in the immature vs. the adult brain. A 4-marker flow cytometry panel and immunolabeling for Nestin/Ki-67/Mash1 showed increases in NSCs as well as in 2 classes of multipotential progenitors. BrdU+/DCX+ cells were increased in the ipsilateral SVZ and parenchyma adjacent to the lesion 14 days after rat CCI. However, very few new mature neurons were seen in the lesion 28 days after injury. Altogether, our data indicate that although the immature brain is capable of mounting a robust proliferative response to CCI that includes an expansion of primitive NSCs and certain progenitors, these responses do not result in sustained neurogenesis or significant neuronal replacement.

Introduction

Pediatric Traumatic Brain Injury (TBI) is a significant problem that affects 600,000 children under the age of 14 each year. Approximately 60,000 of these children require hospitalization and estimates are that 7,400 children die each year from TBI-related injuries.[1] The estimated financial burden of pediatric TBI is $1 billion/year in hospital costs alone.[2] Given this enormous financial burden in addition to the emotional problem placed on caregivers, there is strong rationale for additional studies of pediatric TBI. Due to the fact that the young nervous system possesses a greater ability to recover from injury than the adult nervous system in general and also in response to mechanical brain injuries, it is informative to study those properties of the immature brain that allows for greater recovery.[3-5]

The Subventricular Zone (SVZ) is a mosaic of neural precursors that includes multipotential neural stem cells (NSCs), bipotential progenitors and unipotential progenitors.[6] Virtually all of the neurons and glia that populate the mature brain arise from neural precursors (NPs) that reside in germinal zones immediately adjacent to the lateral ventricles during development. The SVZ achieves its maximal size and heterogeneity during the neonatal period when the brain is in a dynamic state of development. With the recent discovery that adult olfactory bulb neurogenesis in the human brain likely ceases after 18 months of age, there is increased interest in studying the neural precursors (NPs) of the neonate.

Changes in SVZ cell proliferation have been extensively examined across a number of adult animal models of traumatic brain injury including penetrating brain injuries, aspiration lesions, fluid percussion injury and controlled cortical impact (CCI).[7-11] Studies to date have revealed injury model dependent differences in the SVZ proliferative responses. In rats, the total number of cells in the adult SVZ increases 1 week following aspiration lesions of the somatosensory cerebral cortex.[12] In the fluid percussion injury model in adult rats, the number of 5-bromo-2-deoxyuridine (BrdU)-labeled SVZ cells increases 2 and 4 days after injury.[8] In the CCI model, short term increases in proliferation were seen in adult rats[13, 14] The dorsal aspect of the ipsilateral SVZ to the injury is the area of the SVZ most involved in proliferation following injury and has also been characterized in the adult mouse after CCI.[11] Therefore, it has been well established that the adult SVZ is capable of mounting a robust proliferative response to a variety of mechanical traumatic brain insults.

Whereas cells born in the ventricular zone and SVZ of the developing forebrain migrate towards many nuclei, neuroblasts in the intact adult SVZ of most vertebrates migrate primarily to the olfactory bulb along the rostral and medial migratory streams.[15, 16] While this appears to be the case in the intact brain, a number of studies indicate that brain injury can induce SVZ cells to migrate more broadly, especially towards the lesion. Using BrdU labeling, newly generated neurons can be followed and shown to express both early markers, such as Doublecortin (Dcx) as well as markers of more mature neurons such as Class III beta tubulin, calretinin or NeuN. Additional studies have been performed using retrograde labeling to provide evidence that these new neurons are indeed integrated into neural circuits.[17] In our studies of neonatal hypoxic-ischemic brain injury, we have documented the significant production of new neurons from the SVZ that begins a few days after the injury and persists for at least 2 months.[18, 19] To date, no studies have examined if similar increases in SVZ proliferation and regeneration occur following focal, mechanical traumatic brain injury in pediatric-aged rodents. As studies of traumatic injury in adult rats have rarely seen migration of SVZ cells into the neocortex, we hypothesized that the production of new neocortical neurons would be greater in the immature brain.

We recently established a novel flow cytometry protocol to quantify the relative proportions of 8 unique SVZ progenitors as well as NSCs.[6] This powerful tool allows us to examine the effects of injury and other genetic manipulations on SVZ cells with a greater level of resolution previously unattainable. We have applied this method to compare the composition

of SVZ cells between wild-type and genetically altered mice, as well as in a mouse model of hypoxia-ischemia.[20]

In the studies reported here, we used several complementary approaches to evaluate changes in the SVZ NSC and progenitor responses subsequent to pediatric TBI. We used CCI to equivalently damage the somatosensory cortex of rats at postnatal day 6 (P6), P11 and P17 and P60. The P6 time point was chosen to allow a direct comparison with our studies of hypoxic-ischemic injury; the P11 animal was chosen to model injury to neonates, the P21 rat was chosen to model traumatic injury in toddlers and the P60 rat was chosen to model injury in adults. In addition, we modified the CCI model to produce a similar injury in P14 mouse. Using these injury paradigms, we evaluated cell proliferation within the SVZ following CCI, characterized which populations were changing following injury and compared the regenerative potential across this range of ages. These studies reveal that the developing brain mounts a much more robust proliferative and regenerative response to focal TBI than the adult brain, which arises from the expansion of NSCs and specific subsets of progenitors in the SVZ.

Materials and Methods

Reagents

Common laboratory chemicals were purchased from either Sigma (Sigma, St. Louis, Mo., USA) or VWR International (Radnor, PA). Cell culture media were purchased from either Invitrogen or Sigma. Recombinant EGF and FGF2 were purchased from PeproTech, Rocky Hill, NJ, USA. Optimal cutting temperature compound embedding medium was purchased from Sakura Finetek, Torrance, CA, USA. The following antibodies were used for our studies: Rat anti-BrdU (1/30, Accurate Chemicals, Westbury, N.Y., USA); mouse anti-Mash1 (BD Pharmingen San Jose, CA, USA, www.bdbiosciences.com; 1:50); chicken anti-Nestin (Aves Labs Inc. Tigard, OR, USA, www.aveslab.com; 1:250); rabbit anti-Ki-67 (Vector, Burlingame, CA, USA, www.vectorlabs.com; Z0311, 1:500); mouse anti-NeuN (Millipore/Chemicon, Billerica, MA, USA, www.chemicon.com; 1:100), mouse anti-HuC/D (Invitrogen, Grand Island, NY, USA, www.invitrogen.com; 1:50). The following secondary antibodies were used: RedX-conjugated donkey anti-rat; Alexa 488 conjugated-donkey anti-rabbit, Alexa 549-conjugated donkey anti-chicken and AMCA-conjugated donkey anti-mouse (1/200, all from Jackson ImmunoResearch, West Grove, Pa., USA). 4',6'-diamidino-2-phenylindole (DAPI) was purchased from Sigma. Fluoro-Gel was purchased from Electron Microscopy Services, Hatfield, PA, USA.

For surface marker analysis by flow cytometry the following antibodies were used: antibodies against Lewis-X-Alexa Flour 488 (1:20, LeX/CD15, MMA; BD Bioscience, San Diego, CA), CD133-APC (1:50,13A4; eBioscience, San Diego, CA), CD140a-PE (1:400, APA5; BioLegend) and NG2 Chondroitin Sulfate Proteoglycan (1:100, AB5320; Millipore); goat anti-rabbit IgG Alexa Fluor 700 (1:100; Invitrogen). Ultrapure formaldehyde was purchased from Polysciences, Inc; Warrington, PA.

Controlled Cortical Impact

All experiments were performed in accordance with protocols approved by the institutional animal care and use committee of the University of Rutgers-New Jersey Medical School. Timed pregnant Sprague Dawley rats (Charles River, Wilmington, Del., USA) and timed pregnant C57Bl/6 mice were housed and cared for by the Department of Comparative Medicine. Unilateral CCI was performed on the somatosensory cortex of postnatal day 6 (P6), P11, P17 and P60 rat pups and on P14 mouse pups. The pups were anesthetized with ketamine/xylazine. Once fully anesthetized, the scalp was cleansed and an incision along the midline created to expose the skull. In order to produce equivalent injuries among different aged animals and across species, different size impactor tips and depths of injuries were performed (Table 1). Age-matched sham-operated animals only received craniectomies. Animals were placed on heating pads at 37° and monitored continuously for 2 h after surgery. In addition, immediately

after surgery, all animals received 3% body weight of 0.9% saline subcutaneously (SC) to prevent dehydration.

P60 rats were singly caged until they were sacrificed. All other rat age groups and the P14 mouse group were returned to their dam cages to resume nursing with their mothers until they were sacrificed.

BrdU Injections and Intracardiac Perfusions

BrdU was administered intraperitoneal at 50 mg/kg dissolved in 0.007 N NaOH in PBS. Several dosage paradigms were used as described later. For intracardiac perfusions, animals were anesthetized with a mixture of ketamine (75 mg/kg) and xylazine (5 mg/kg) and then fixed by intracardiac perfusion with media followed by 3% paraformaldehyde in PBS 4 hours following the final BrdU injection. Each brain was removed from the skull, post-fixed overnight and then cryoprotected for 24 h in 30% sucrose in water. The brains were frozen in optimal cutting temperature compound embedding medium on a dry-ice/ethanol slush.

Immunofluorescence

Immunofluorescence was performed on 40 μm sections as previously described.[5] After secondary antibody incubation the sections were washed, counterstained with 1 μg/ml DAPI for 5-10 minutes, and coverslipped with Fluoro-Gel. The sections were analyzed using an Olympus AX70 fluorescence microscope equipped with a Q-imaging CCD camera and IPLab imaging software. All secondary antibody combinations were carefully examined to ensure that there was no bleed through between fluorescent dyes or cross-reactivity between secondary antibodies. No signal above background was obtained when the primary antibodies were replaced with pre-immune sera.

Quantification of Proliferation

To quantify BrdU labeled cells to obtain a mitotic index, six sections were sampled at 150 μm intervals per brain. The dorsolateral SVZ was divided into three distinct anatomical subregions as previously described.[21] Briefly, the medial region consists of the densely packed SVZ cells immediately adjacent to the ependymal layer. The mediolateral region is approximately 200 μm lateral from the medial region and is much less dense than the medial region. Finally, the lateral SVZ is 200 μm lateral to the mediolateral region and consists of densely packed cells. Two fields per SVZ region were assessed per section (ipsilateral and contralateral to the injury site). Each field occupied an area of 50μm^2. The numbers of BrdU+ and total DAPI+ cells in each region of the damaged neocortex were then quantified and averaged. The data are presented as the percentage of labeled cells per field after correction using the Abercrombie correction as described in greater detail in a previous publication.[22]

For stereological evaluation of triple Immunofluorescence labeled specimens, 40 μm sections were analyzed using the MicroBrightfield StereoInvestigator program on an Olympus BX51 microscope. [23 2222] Six sections were sampled at 150 μm intervals per brain. For each section, quantification of Nestin+/Ki-67+/Mash1- stem cells and Nestin+/Ki-67+/Mash1+ intermediate progenitors was conducted in the medial, mediolateral and lateral subregions of the SVZ as described above. Six fields of 50 μm^2 were assessed per section in the ipsilateral and contralateral SVZ. The numbers of Nestin+/Ki-67+/Mash1- and Nestin+/Ki-67+/Mash1+ cells in each region of the damaged neocortex were then quantified, averaged and then converted to cells/mm^3.

Neurosphere Propagation and Quantification

Neural stem cells and neural precursors from the SVZ of CCI, sham operated and untouched treated animals were harvested and grown in culture as neurospheres. Two days after CCI injury to the somatosensory cortex was performed on male Sprague Dawley rats at

P11. The animals were sacrificed by decapitation and their brains immediately removed for SVZ dissection as previously described [24]. Briefly, a 3 mm thick coronal section of the brain was obtained by cutting 2mm and 5mm from the rostral end of the brain and placed in cold PGM [(PBS, 1mM $MgCl_2$ and 0.6% dextrose in PBS). The hippocampus, the corpus callosum and meninges were removed and a wedge of brain tissue between 1 o'clock and 3 o'clock enclosing the cortex and ventricle containing the SVZ was excised. The tissue was digested enzymatically with a mixture containing 0.25% trypsin/EDTA, 100 units Papain, 250 µg/ml of DNase I and 3 mM MgSO4 in DMEM/F12. The reaction was stopped with trypsin inhibitor in chemically defined medium ProN [DMEM/F12, B27 supplement, 50 ug/ml apotransferrin and 50 ug/ml gentamicin (50 ug/ml)]. The tissue was triturated to obtain a single cell suspension, collected by centrifugation and counted with a hemocytometer. Dissociated cells were seeded in 12-well culture plates at a density of $5x10^4$ cells/mL in ProN media containing 20 ng/ml EGF and 10 ng/ml FGF–2. Cultures were fed every 2 days by replacing half of the media with an equal volume of fresh media. Neurosphere numbers were quantified after 7 days in vitro as described previously[25]. Briefly, six random fields per well in quadruplicate were imaged in phase contrast with a 10x objective. Neurospheres of at least 25 μm in diameter were counted and a total of 24 photos per condition were analyzed. Neurosphere diameters were determined from the same images using a microscale with 10 μm subunits as reference.

Flow Cytometry

C57BL/6 pups at 2 days recovery after CCI (P16) were decapitated and the contralateral and ipsilateral SVZs from injured brains, as well as SVZs from sham-operated animals and untouched control animals were isolated by microdissection and placed in dishes containing cold PGM. SVZs were pooled and incubated with 0.45 Wünsch unit /ml of Liberase DH (Roche) and 250 µg of DNase1 (Sigma) in PGM and were shaken at 230 rpms (Innova 2300, New Brunswick Scientific, Edison, NJ) at 37°C for 30 min. Enzymatic digestions were quenched with 10 ml of PGB (PBS without Mg^{2+} and Ca^{2+} with 0.6% dextrose and 2 mg/ml fraction V of BSA-Fisher) and cells were centrifuged for 5 min at 200 xg. Cells were dissociated by repeated trituration, collected by centrifugation, counted with a hemocytometer and diluted to at least 10^6 cells per 50 µl of PGB. All staining was performed in 96 V-bottom plates using 150 µl volume. For surface marker analysis, cells were incubated in PGB for 25 min with antibodies against Lewis-X, CD133-APC, CD140a, and NG2 Chondroitin Sulfate Proteoglycan. Cells were washed with PGB by centrifugation at 278 xg. Secondary antibody Goat anti-rabbit IgG Alexa Fluor 700 was used to detect NG2. Cells were incubated with secondary antibodies and DAPI (1:3000, Invitrogen) in PGB for 20 min and then washed by centrifugation in PGB at 278 x g. Cells from SVZ were fixed with 1% ultrapure formaldehyde for 20 min, collected by centrifugation for 9 min at 609 x g, resuspended in PGB and stored at 4°C overnight. All sample data were collected on a BD LSR II (BD Biosciences Immunocytometry Systems). Matching isotype controls for all antibodies were used and gates were set based on these isotype controls. Data were analyzed using FlowJo software (Tree Star, Inc; Ashland, OR).

Statistical Analyses

Results from the cell counts were analyzed for statistical significance using ANOVA followed by Tukey's post hoc test. All data are presented as means ± SEM. Comparisons were interpreted as significant when associated with $p < 0.05$.

Results

Measuring the SVZ Response to Pediatric CCI

The neurosphere has remained a standard assay for measuring numbers of neural stem cells in the SVZ, therefore, we isolated SVZ cells from CCI treated and control animals to determine whether there was an increase in the number of sphere-forming cells after CCI in P11 rats. Neurosphere cultures from ipsilateral and contralateral SVZs of CCI injured animals and from SVZs of sham operated and naive control animals were established two days after CCI (Figure 1 A). Spheres were propagated in chemically defined medium (ProN) supplemented with EGF and FGF-2. After 7 days *in vitro*, the number of neurospheres formed from the ipsilateral SVZ after CCI was 157% higher than the contralateral side ($p<0.001$), 260% higher than the sham operated ($p<0.001$) and 390% higher than the naïve SVZ ($p<0.001$) (Figure 1B). There was no significant difference in the number of neurospheres generated from the contralateral SVZ compared with the sham operated control and the naïve SVZ, and no significant differences between neurosphere number formed from sham operated and naïve SVZ (Figure 1B).

The size of a neurosphere can be indicative of the proliferative capacity of the precursors within it. Therefore, we measured the diameter of at least 20 neurospheres from each condition. The size of the neurospheres obtained from the ipsilateral hemisphere of the injured brain was 48% larger than the contralateral SVZ ($P<0.001$), 110% larger than the sham operated SVZ ($P<0.001$) and 122% larger compared with neurospheres from the naive SVZs. No significant differences were found in the sizes of neurospheres generated from the contralateral SVZ compared with the sham operated control and the naïve SVZ, and there were no significant differences in neurosphere size formed from sham operated vs. naïve SVZ (Figure 1C).

In vivo Response of the Rat SVZ to CCI

We next examined the effects of pediatric CCI had on the SVZ cells in situ. To determine whether there were differences in the proliferative responses as a function of age, we needed to reliably produce comparable injuries across ages. Using the 2.5 mm diameter impactor tip that was optimal for P11 rats and driving it to the same depth (1.25 mm) created a massive deeper injury in P6 animals that was not large enough or deep enough in P17 or P60 rats. Therefore, we adjusted the size of the impactor tip and depth it traveled past the zero point relative to the size and age of the animals to create comparable injuries (Table 1). The force (4m/s) and dwell time of the impactor tip (150ms) remained constant for all animals and age groups. Each injury was centered over the sensorimotor cortex, which depending on the age, is located ~1 to 2 mm posterior to bregma and ~ 1 to 1.5 mm lateral to the midline. The different impactor diameters created similar lesions that spanned the entire rostral to caudal extent of the SVZ. By 4 days of recovery, the lesion cavities were free of debris and were relatively similar in size and depth among all age groups (Supplemental Figure 1).

To evaluate changes in SVZ cell proliferation in situ, animals received BrdU, which labels cells in the S phase of the cell cycle. Rats were subjected to CCI on P6, P11, P17 and P60 and i.p. injections of BrdU were administered once daily on days 1–4 of recovery. Four hours after the last BrdU injection the animals were perfused and the brains processed for histology. Immunofluorescence microscopy for BrdU revealed a strong ipsilateral proliferative response in animals injured at P6, P11 and P17 (Figure 2b, d, f). In contrast, the proliferative response in the SVZ of P60 rats was similar to sham-injured controls (Fig. 2h, I). A quantitative analysis of the ratio of BrdU-labeled cells to total cells (mitotic index) revealed that the response to the CCI at P6 was significantly increased in all 3 SVZ sub regions in the ipsilateral hemisphere, with approximately 30-40% BrdU+ cells in each SVZ region compared to 10-20% of cells in the contralateral hemisphere and in sham-operated controls (Fig. 2i). Animals injured on P11 again exhibited a unilateral increase in BrdU+ cells on the ipsilateral side; however, this increase was only seen in the medial region of the SVZ (Fig. 2j). BrdU+ cells were less abundant in the P11 animals compared to P6 animals, and the fold increase after injury was

also reduced. Interestingly animals injured on P17 exhibited a bilateral increase in proliferating cells to CCI that was most pronounced in the mediolateral and medial aspect of the SVZ in both hemispheres (Fig 2e, k). This increased bilateral response was not seen in the lateral SVZ region in either hemisphere after CCI at P60 when compared to sham-operated controls (Fig. 2l). These data closely coincide with our previously published data showing that the proliferative response in the rat SVZ after cryoinjury model, is age-dependent.[26]

Identity of Proliferating Rat SVZ Cells Following CCI

Our data on the proliferative response to CCI in the SVZ does not provide information on the cell types proliferating. While our data from the neurosphere assay suggested that NSCs were proliferating in response to the pediatric CCI, neural progenitors as well as NSCs can also generate neurospheres. Therefore, to more accurately characterize the identity of the proliferating SVZ cells following CCI, we performed immunostaining of brain sections with antibodies against Nestin, Mash1 and Ki67 and stereological cell counts were performed. Labeled cells that were Nestin+/Mash1+/Ki-67+ were characterized as multipotential progenitors whereas Nestin+/Mash1-/Ki-67+ cells were characterized as NSCs. CCIs were performed on P11 and P17 and 4 days post injury animals were perfused and their brains immunostained. By high power epifluorescence microscopy, we observed that the Nestin+/Mash1-/Ki-67+ cells preferentially resided immediately adjacent to the ependymal cells in the medial aspect of the dorsolateral SVZ (Fig. 3B). By contrast, Nestin+/Mash1+/Ki-67+ multipotential progenitor cells were found throughout the SVZ (Fig. 3C). At 4 days after CCI, the number of Nestin+/Mash-1-/Ki67+ cells immediately adjacent to the ependymal layer was significantly increased ($p < 0.01$) over naïve and sham controls (Fig. 3A) in the ipsilateral hemisphere compared to controls (Fig. 3D). There was a trend for an increase of Nestin+/Mash1-/Ki-67+ NSCs in the contralateral medial SVZ, but this increase did not achieve statistical significance (Fig. 3D). The numbers of Nestin+/Mash1+/Ki-67+ multipotential progenitors were unchanged in the medial SVZ, but increased significantly in the lateral tip of the ipsilateral SVZ ($p < 0.01$) (Fig. 3E, F). Again, there was an increase in the Nestin+/Mash1+/Ki-67+ cells in the contralateral lateral SVZ (Fig. 3F), but this difference did not reach statistical significance(Fig. 3F). These results indicate that pediatric CCI more robustly stimulated the proliferation of multipotential progenitors than NSCs.

Rat Neurogenesis

To determine whether these newly generated precursors contribute to neuronal replacement after pediatric CCI, we performed staining of doublecortin (DCX), a microtubule-associated protein that is regularly used as a marker for neuroblasts. Rats were subjected to CCI on P11 and i.p. injections of BrdU were administered once daily on days 3–5 of recovery. The animals were perfused for histology either 14 days or 28 days after injury. Staining for DCX revealed a robust increase in DCX expression in the ipsilateral hemisphere compared to the contralateral hemisphere (Fig.4A, B). There also was strong increase in bipolar, cells that were DCX+/BrdU+ whose processes were oriented either parallel to or perpendicular to the lesion in the ipsilateral hemisphere of injured animals compared to controls and the contralateral hemisphere 14 days after injury (Fig. 4C).

We then asked whether the increase in neurogenesis caused by CCI persisted and resulted in the production of mature neurons using the markers NeuN and HuC/D. Animals that had received BrdU injections as described above were sacrificed 28 days post injury and stained for BrdU and NeuN or HuC/D. Whereas there had been numerous BrdU+/DCX+ cells present at 14 days of recovery, there were very few BrdU+/DCX+ cells remaining at 28 days of recovery and contrary to our hypothesis, BrdU+/NeuN+ and BrdU+/HuC/D+ cells were extremely scarce in the cortex surrounding the lesion site. There were fewer than 1 double positive cell per 6 sections in each of 3 brains analyzed (Fig. 4D). We attempted to determine

whether DCX+ cells were dying by staining for active caspase-3; however, we were unable to find any DCX+/active caspase-3+ cells (data not shown).

Proliferative Response of the SVZ Following CCI in the Immature Mouse

Limited markers are available presently to characterize the variety of precursors present in the rat SVZ. Therefore, we decided to develop a comparable pediatric CCI model in the mouse to enable us to apply our recently developed 4-marker flow cytometry panel that has the capability of identifying and quantifying the relative abundance of 8 distinct SVZ neural precursors.[6] Adjusting for gestation times, mice are generally at the same level of development as rats three days later, i.e. P11 rats are roughly equivalent to P14 mice. Therefore, based on the results above, we developed a CCI injury paradigm for P14 mice. Again, we adjusted the size of the impactor tip (1.5 mm) and the depth it traveled from the zero point (0.7 mm) to produce an equivalently sized injury to those produced in the rat (Fig. 5A) Animals were sacrificed 2 days post injury and stereological cell counts of proliferating Ki-67+ cells and total DAPI+ cells in the three SVZ subregions were conducted. There was a strong bilateral response in both SVZs in all three subregions, with the most lateral SVZ subregion showing the most prominent increase in proliferation over sham-operated and untouched naïve animals seen in the lateral SVZ (Fig. 5B).

Identifying Proliferating SVZ Cell Populations Using Flow Cytometry

. Flow cytometry was performed at 24 h after CCI to P14 mice. This analysis revealed a three-fold increase in the NSCs (CD133+/LeX+/NG2-/CD140a-) in the ipsilateral SVZ and a two-fold increase in the contralateral SVZ compared to sham-operated and untouched controls (Fig. 6). CCI also had a bilateral effect on the CD133+/LeX+/NG2+/CD140a-, “multipotential-2” cells (MP2s), which were increased four times to the levels seen in sham-operated and untouched controls. There were also 2-fold increases in the numbers of CD133-/LeX-/NG2+/CD140a-, which correspond to a heterogeneous pool of “glial restricted progenitor-2s and MP3s” vs. the contralateral hemisphere. The percentages of CD133-/LeX+/NG2-/CD140a-, MP1 cells and CD133-/LeX+/NG2+/CD140a+ “PDGF and FGF responsive multipotential progenitors” (PFMPs) were decreased 3-fold in the ipsilateral hemisphere and 2-fold in the contralateral hemisphere (Fig. 6).

Discussion

The CCI brain injury models employed in these studies utilized different size CCI impactor tips which travel at differing depths at a constant velocity and dwell time to create mechanical injuries in pediatric-aged and adult rat and mouse somatosensory cortices. Our data show that 1) The pediatric brain possesses a greater inherent ability to regenerate in comparison to adult brains after comparable CCI injuries; 2) The injured SVZ produces more neurospheres that grow at an accelerated rate; 3) Unilateral CCI produces a robust response in the contralateral SVZ, especially at P17; 4) There is an increase in the numbers of proliferating Nestin+/Mash-1- precursors in the ipsilateral SVZ; 5) By flow cytometry there is an increase in NSCs as well as in the MP2s and MP3s, with a corresponding decrease in MP1 and PFMPs 6) Despite these increases in proliferation after injury and increased migrating neuroblasts to the injury site, very little regeneration of mature neurons was seen.

Whereas many studies have evaluated cell proliferation and regeneration in the SVZ after TBI in adult aged animals, fewer studies have evaluated the extent to which these processes are occurring in pediatric-aged animals. Significant self-recovery occurs following all but the most severe episodes of TBI.[23, 27] The mechanisms underlying this remain unclear, though injury-induced neurogenesis is one compelling potential contributor to post-injury recovery.[8, 28] There have been numerous studies that have suggested that the adult brain is capable of mounting an endogenous repair response, thus raising hope that regeneration after brain damage might be stimulated.[12, 29-31] We set out to determine if these endogenous responses were also present in younger animals and to characterize the subsets of precursors that were responding after a controlled cortical impact directly to the somatosensory cortex.

Our data on the proliferative responses to pediatric CCI closely mirror those found in a previous study by Covey et al., 2010 that defined the developing SVZ response to cryo-injury, a less severe and penetrating brain injury model than CCI [26]. They found significant increases in proliferation in the same SVZ regions that we reported here in rats injured on P10 and P17. Also in agreement with our data, they observed a significantly diminished proliferative response as measured via mitotic index in rats injured at 2 months. However, the large contralateral effect we observed in young injured brains, especially those injured at P17, was largely absent in cryo-injury model.

In another brain injury model, aspiration lesion, there are more significant increases in BrdU+ SVZ cells in the adult than seen in our CCI model and studies using the Vannucci model of hypoxia-ischemia on neonatal rats and mice from our lab have showed a very robust proliferative response within the SVZ that persists for months after the injury.[6, 18, 19, 22, 24, 25, 32, 33] One difference between those studies and the present study is that the aspiration lesion and the hypoxia-ischemia injury produces more widespread damage that affects a greater percentage of the injured hemisphere than the focal CCI produces. This suggests that injury signals are produced in the damaged hemisphere and that the larger the injury the greater the stimulus. Not only are injury signals being produced by cells residing in the injured tissue, but immune cells attracted to the wound will produce and release of cytokines and growth factors that are known to affect SVZ cells.[34]

Our study utilized a novel flow cytometry panel to determine which specific types of SVZ cells were being affected by pediatric CCI.[6] The four-marker flow panel we employed provides a large amount of data on the relative percentages of NSCs as well as 7 multipotential and bipotential progenitors. Interestingly, we see a different set of precursors being affected by CCI vs. hypoxia-ischemia. Notably, we find an increase in the proportion of NSCs after CCI injury in the mouse, whereas these cells become less abundant after neonatal H-I [20]. Furthermore, there is a significant expansion of glial precursors after H-I whereas there is not a large amplification of these cells after CCI. However, one similarity is the increase in the MP3/GRP2 cells. Interestingly, these cells are EGF responsive precursors, suggesting that increases in either

EGF ligands or in the expression of the EGFR is responsible for the amplification of these precursors. A limitation to this method as currently implemented is that is not possible to determine whether the shifts in the SVZ population are due to changes in cell proliferation or changes in cell survival, differentiation or a combination of all these parameters.

To date there isn't a reliable flow cytometry panel for the developing rat SVZ; therefore, to characterize the responses of the NSCs and multipotential progenitors after pediatric CCI, we used multi-label immunofluorescence and performed stereological cell counts in the injured brains. Whereas, previous studies have documented increases in Nestin expressing cells throughout the SVZ after injury and increases in Ki-67 and transit amplifying Mash1 type C cells, these markers are widely expressed and cannot be used alone and without positional information to provide unambiguous data[12, 22, 35-38].

Despite the increased ability of pediatric-aged SVZ cells to proliferate and to produce more NSCs and progenitors, our studies showed that these responses ultimately failed to produce new neurons in the injured cortex. We did see a robust increase in SVZ neuroblasts labeled with DCX as well as what appeared to be increased ectopic migration of these cells towards the lesion. Various studies have also shown similar ectopic migration of SVZ-derived neuroblasts to injured areas in the adult brain after aspiration injury, pressure injuries and forms of hypoxic-ischemic injury [14]. In a more recent study, the Szele group quantified the numbers of olfactory bulb neurons produced after TBI and found that neurogenesis in the OB was not diminished by TBI. These results are consistent with a scenario in which those cells that migrate from the SVZ to the area of injury are newly born cells, as opposed to cells that fail to follow their normal migratory routes.[39] Moreover, in their studies, those SVZ cells that emigrated from the SVZ into the neocortex differentiated into astrocytes and oligodendrocytes, but not neurons.[40] Of those cells that adopt a neuronal fate, the vast majority of these new neurons migrated into subcortical regions such as the striatum, or they were trapped in the subcortical white matter.[39] By contrast, in the immature brain, the newly produced neurons can migrate to the neocortex where they can fully differentiate into neurons expressing mature markers.[41, 42] Clearly then, there are constraints to migration that develop as the brain matures. However, reminiscent of these past studies, the pediatric-aged injured brain failed to regenerate new, mature neurons to replace neurons lost to the mechanical injury.

Numerous changes occur in injured brain that can affect the homeostasis of the precursors that reside within the SVZ. Two well-studied signals are KCl and glutamate. Both have both have been shown to enhance the proliferation of immature cells.[43-45] In addition, the injured brain activates both astrocytes and microglia, which are both known to secrete a variety of growth factors as well as immune modulators that may affect progenitor proliferation and survival. [46-48]. Also, the progenitor cells themselves make physical contact with the vasculature to direct some of these effects.[49] Thus, the mechanisms underlying TBI-induced neurogenesis are likely not straightforward nor easily worked out, and therefore remain compelling targets to study. Understanding why the young brain has a stronger proliferative response than the adult brain is a very important goal. Future studies can exploit those differences to induce greater cell production after adult injury.

Acknowledgements: This research was supported by grant # 09-3207-BIR-E-2 from the New Jersey Commission on Brain Injury Research awarded to SWL.

Table 1.

Animal and Age of Injury	Impactor Tip Size	Depth	Dwell Time	Velocity
P14 Mouse	1.5 mm	0.7 mm	150 ms	4 m/s
P6 Rat	2.0 mm	1.0 mm	150 ms	4 m/s
P11 Rat	2.0 mm	1.25 mm	150 ms	4 m/s
P17 Rat	2.0 mm	1.5 mm	150 ms	4 m/s
P60 Rat	2.5 mm	2.0 mm	150 ms	4 m/s

Table 1: Summary of different CCI impactor tips and depths used to create equivalent size lesions to the somatosensory cortex of mice and rats at 5 different ages.

Figures and Legends

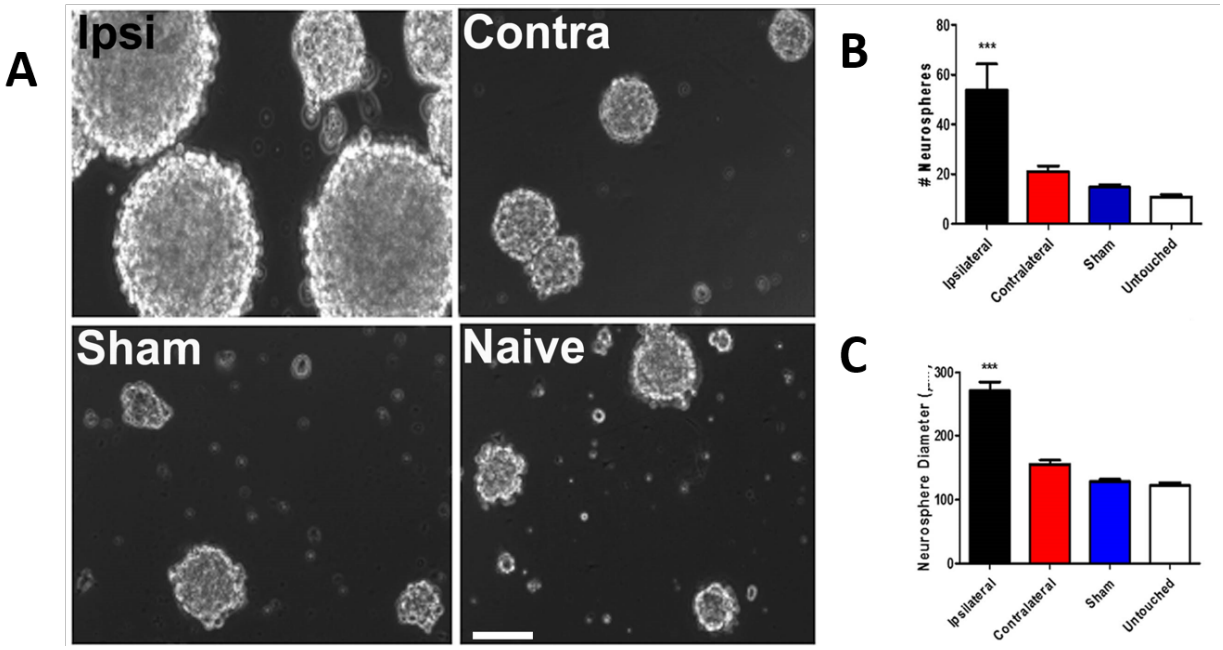

Fig. 1: **Neurosphere number and size increase following traumatic brain injury**

(A) Phase contrast images of neurospheres generated from ipsilateral, contralateral, sham – operated and untouched control SVZs 2 days after CCI and cultured for 7 DIV in a chemically defined medium supplemented with EGF (20 ng/ml) and FGF-2 (10 ng/ml). Scale bar represents 50 µm. (B) Quantification of average neurosphere number obtained per 50,000 SVZ cells seeded in each experimental group. A total of 150-700 spheres were analyzed per condition. Values represent means ± SEM. *** $p<0.001$ by Tukey's post hoc test. n = 6. (C) Quantification of neurosphere diameter obtained in each experimental group. 20 random chosen photos were analyzed per condition. Values represent means ± SEM. *** $p<0.001$ by Tukey's post hoc test. n = 6. Data are representative of at least 3 independent experiments.

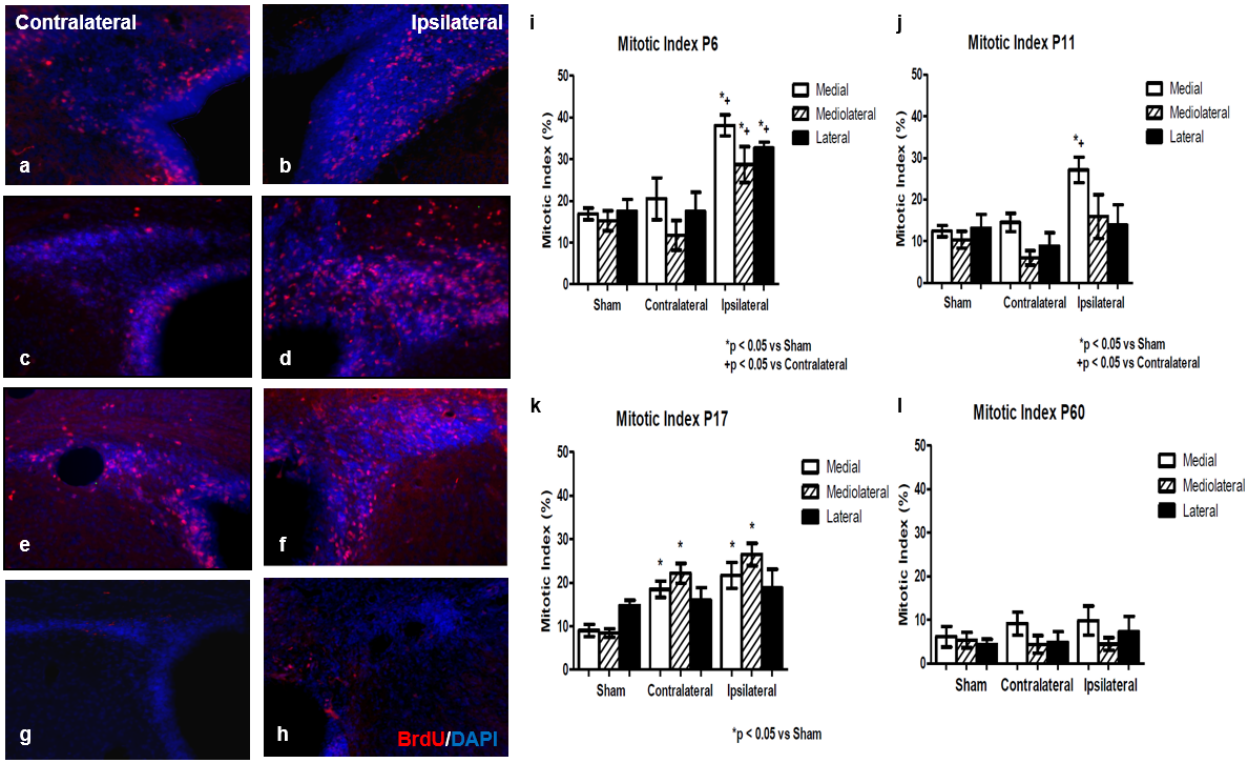

Fig. 2 **Proliferation within the Rat SVZ following CCI.** Representative images of the SVZ showing robust proliferation after CCI at P6 (a, b), P11 (c, d), P17 (e, f) and P60 (g, h). Cell proliferation varied with the age animals received the CCI. Significant increases in the mitotic index of the ipsilateral SVZ compared with the contralateral and sham SVZ were seen in (i) P6 and (j) P11 injured brains. Only (k) P17 brains showed an overall average increase in proliferation in the contralateral hemisphere that was comparable to ipsilateral levels. The mitotic indices in (l) P60 injured brains were not statistically different between hemispheres or sham controls. Values represent means ± SEM. $p<0.05$ IL vs. CL by Tukey's post hoc test. n = 6

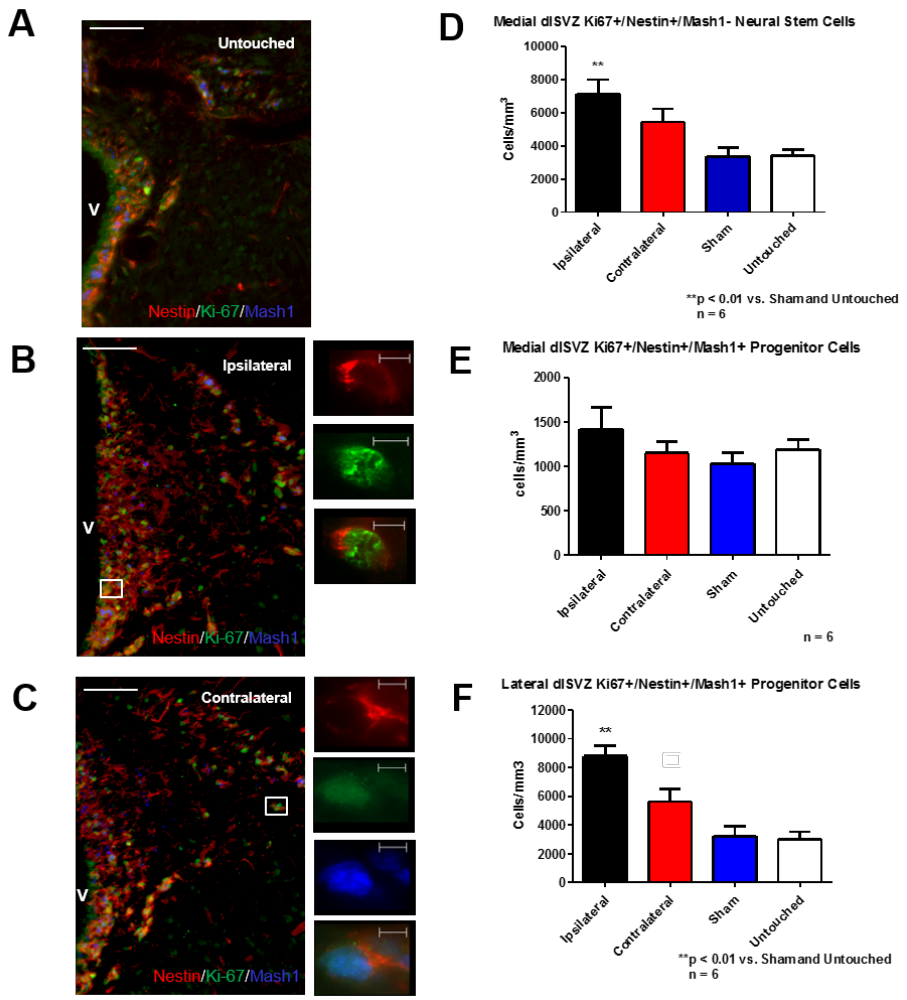

Fig. 3 **CCI altered the numbers of Specific Populations of Rat NSCs and Multipotential Progenitors. (**A) Representative coronal section showing the dorsolateral SVZ from a naïve uninjured P15 rat brain. (B) Representative coronal section of the ipsilateral SVZ from a rat injured on P11 and sacrificed four days after injury showing extensive Nestin, Ki-67 and Mash1 staining throughout the SVZ. Scale bar = 50 µm. High magnification images of boxed region shows a Nestin+/Ki-67+/Mash1- proliferating NSC in the medial SVZ immediately adjacent to the ependymal layer. Scale bars = 10 µm (C) Representative coronal section of the contralateral SVZ , from a rat injured on P11 and sacrificed four days after injury. High magnification images of boxed region shows a Nestin+/Ki-67+/Mash1+ proliferating multipotential progenitor cell in the lateral SVZ. (D) Quantification of stereological cell counts of Nestin+/Ki-67+/Mash1- proliferating NSCs in the medial SVZ. ** Indicates significant increase of double labeled cells in the ipsilateral medial SVZ compared to untouched and sham ($p<0.01$). (E) Quantification of stereological cell counts of Nestin+/Ki-67+/Mash1+ proliferating multipotential progenitors in the medial SVZ. No significant differences were seen between groups. (F) Quantification of stereological cell counts of Nestin+/Ki-67+/Mash1+ proliferating multipotential progenitors in the lateral SVZ. **Indicates significant increase of triple labeled cells in the ipsilateral lateral SVZ compared to untouched and sham controls ($p>0.01$).

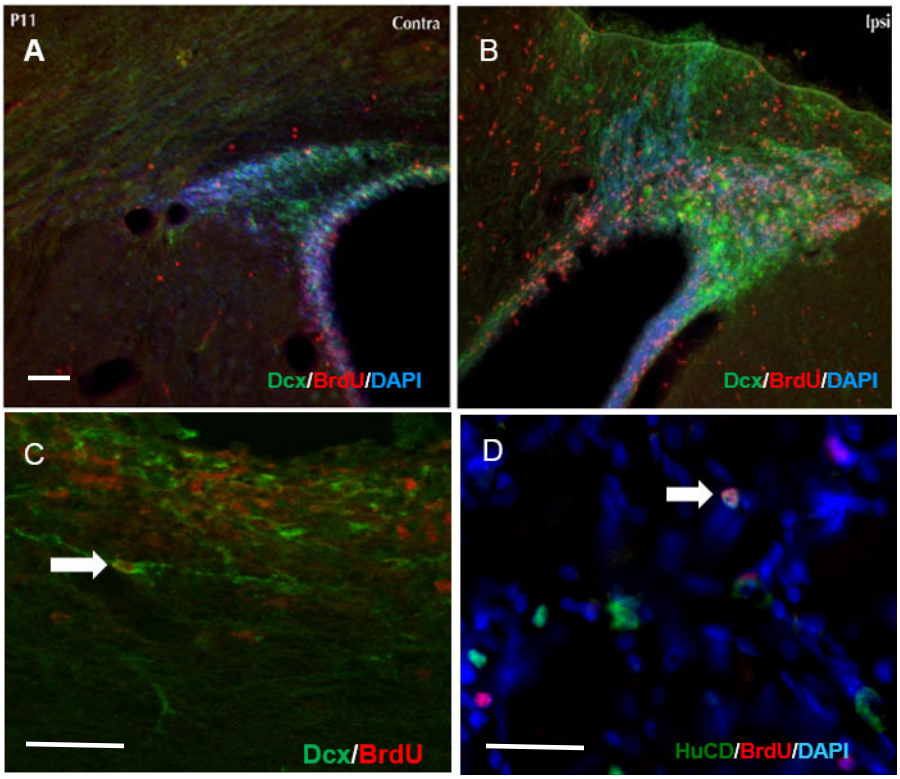

Fig. 4: **Injury induced neurogenesis in neocortex**. P11 animals were administered BrdU on days 4-6 after injury. Epifluorescence images of 40 µm sections from contralateral (A) and ipsilateral (B) SVZs 14 days after injury stained for Doublecortin (DCX) and BrdU. Scale bar represents 100 µm. (C) Confocal image shows co-localization of BrdU and DCX in cells (arrow) adjacent to injury site. Scale bar = 30 µm (D) Confocal image of a brain section from 28 days after recovery shows co-localization for BrdU and the mature neuronal marker HuC/D in a cell (arrow). Scale bar represents 30 µm.

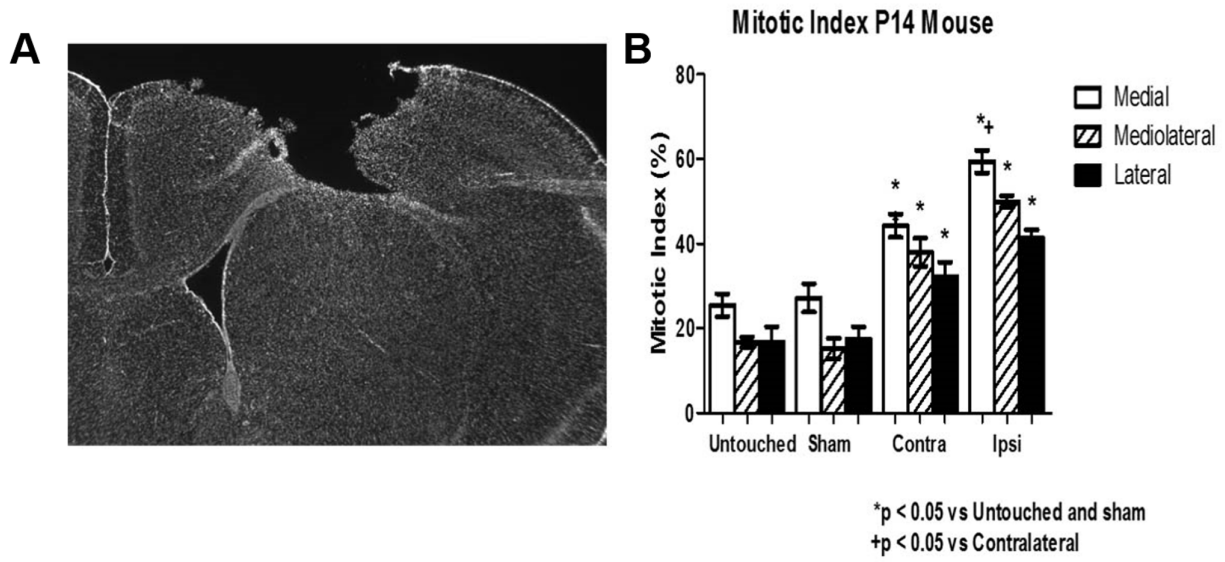

Fig. 5: **Pediatric Mouse CCI and proliferation following injury. (**A) Representative coronal section of mouse brain injured at P14 and sacrificed 4 days after injury. A 1.5 mm impactor tip was used at a depth of 0.9mm to create the injury. The depth and size of the resulting lesion is comparable to the lesions produced in rats 4 days after injury at various ages seen in Figure 3. (B) Quantification of mitotic indices for the ipsilateral, contralateral, sham and untouched control SVZs following BrdU pulses after CCI. Sham surgeries did not produce a proliferative response that was significantly different from untouched controls. Significant increases in percentage of BrdU cells increased significantly in both the ipsilateral and contralateral SVZs following CCI. Values represent means ± SEM. $p<0.05$ IL vs. CL by Tukey's post hoc test. n=6

	NSC	MP1	MP2	MP3/GRP2	PFMP	BNAP/GRP1*	GRP3	Other
	CD133+ LeX+ NG2- CD140a-	CD133- LeX+ NG2- CD140a-	CD133+ LeX+ NG2+ CD140a-	CD133- LeX- NG2+ CD140a-	CD133- LeX+ NG2+ CD140a+	CD133- LeX+ NG2+ CD140a-	CD133- LeX- NG2+ CD140a+	
Untouched	0.91% ± 0.10	16.36% ± 0.91	0.35% ± 0.08	20.97% ± 1.01	2.31% ± 0.32	3.35% ± 0.33	2.86% ± 0.12	52.99% ± 2.21
Sham	1.06% ± 0.10	16.60% ± 1.71	0.44% ± 0.07	21.28% ± 1.66	1.90% ± 0.19	3.37% ± 0.57	2.98% ± 0.14	52.37% ± 3.40
Ipsilateral	**2.52% ± 0.33	**6.74% ± 1.65	***1.72% ± 0.16	***50.49% ± 2.39	*0.89% ± 0.22	5.03% ± 0.64	5.36% ± 0.92	27.22% ± 4.29
Contralateral	1.24% ± 0.35	11.30% ± 2.49	***0.95% ± 0.15	28.74% ± 3.68	1.47% ± 0.24	4.06% ± 0.60	5.48% ± 1.25	46.73% ± 4.23

Fig. 6: **Pediatric Mouse CCI increases NSCs and two distinct multipotential progenitors in addition to decreasing other intermediate progenitor populations.** SVZs from WT C57BL/6 mice were analyzed by flow cytometry at 24 h of recovery using fluorescently labeled probes to the following cell surface antigens: CD133/LeX/NG2/CD140a. 50,000 cell events were analyzed per group after excluding debris and dead cell by DAPI. Four injury-matched SVZs were pooled per sample and four samples were analyzed per condition. Data are presented as mean values ± SEM and are representative of three independent experiments. *$p < 0.05$; **$p < 0.01$; ***$p < 0.001$ vs untouched control by Tukey's post hoc test.

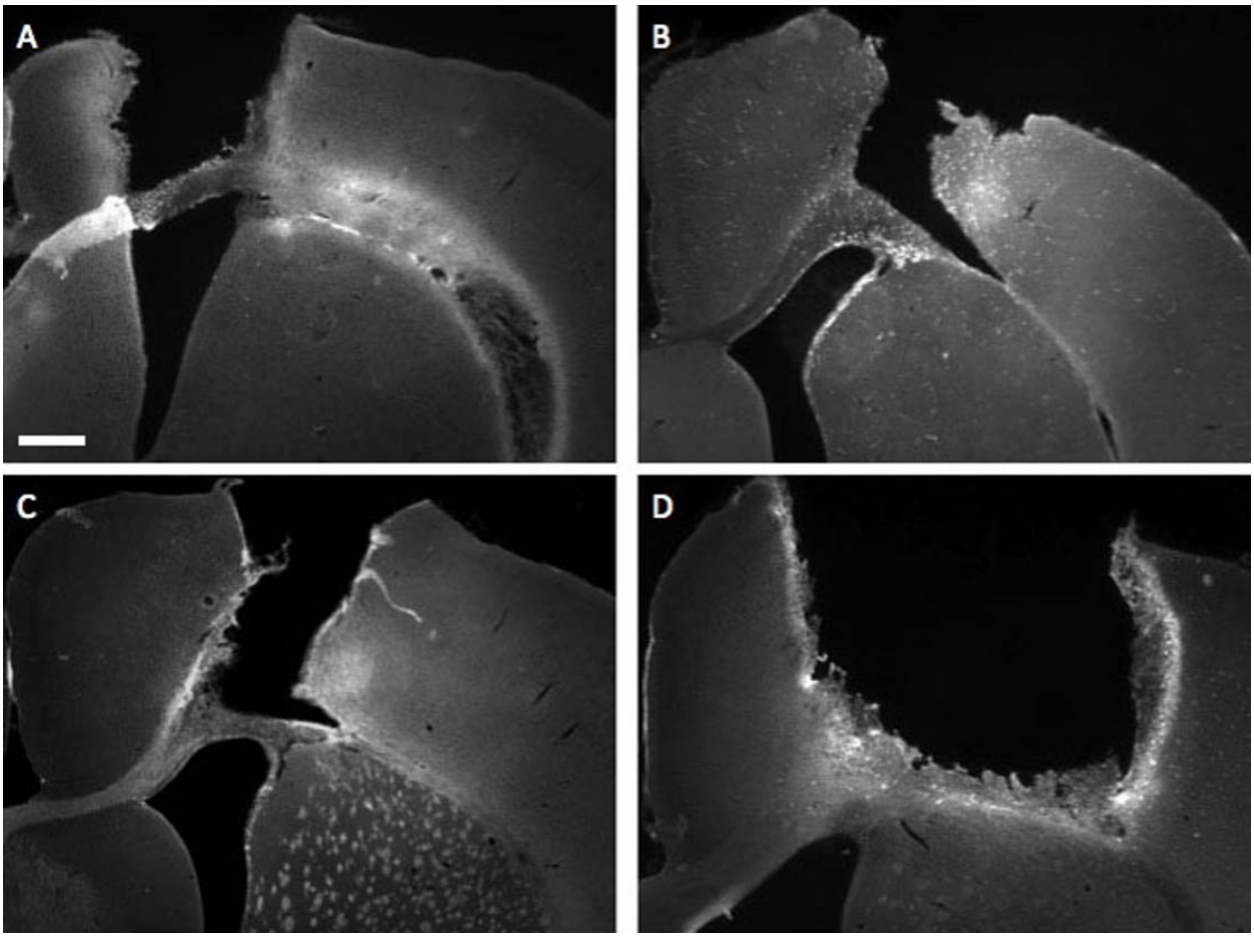

Supplemental Fig 1: **CCI at four different ages showing consistent lesion depth and size in the rat somatosensory cortex.** Velocity (4 m/s) and the duration (150 ms) of the impactor remained constant while the depth of the CCI was altered with age. (A) Injury at P6, 1.00 mm depth, (B) P11, 1.25 mm depth, (C) P17, 1.50 mm depth and (D) P60, 2.00 mm depth. Scale bar = 1 mm.

References Cited

1. Keenan, H.T. and S.L. Bratton, (2006) Epidemiology and outcomes of pediatric traumatic brain injury. Dev Neurosci. **28**(4-5): p. 256-63.
2. Schneier, A.J., et al., (2006) Incidence of pediatric traumatic brain injury and associated hospital resource utilization in the United States. Pediatrics. **118**(2): p. 483-92.
3. Kennard, M.A., (1959) Behavior problems and the brain injured child. Northwest Med. **58**: p. 1535-41.
4. Sun, D., et al., (2005) Cell proliferation and neuronal differentiation in the dentate gyrus in juvenile and adult rats following traumatic brain injury. J Neurotrauma. **22**(1): p. 95-105.
5. Covey, M.V., et al., (2010) Defining the critical period for neocortical neurogenesis after pediatric brain injury. Developmental Neuroscience. **32**(5-6): p. 488-98.
6. Buono, K.D., et al., (2012) Leukemia inhibitory factor is essential for subventricular zone neural stem cell and progenitor homeostasis as revealed by a novel flow cytometric analysis. Dev Neurosci. **34**(5): p. 449-62.
7. Urrea, C., et al., (2007) Widespread cellular proliferation and focal neurogenesis after traumatic brain injury in the rat. Restor Neurol Neurosci. **25**(1): p. 65-76.
8. Chirumamilla, S., et al., (2002) Traumatic brain injury induced cell proliferation in the adult mammalian central nervous system. J Neurotrauma. **19**(6): p. 693-703.
9. Kleindienst, A., et al., (2005) Enhanced hippocampal neurogenesis by intraventricular S100B infusion is associated with improved cognitive recovery after traumatic brain injury. J Neurotrauma. **22**(6): p. 645-55.
10. Rice, A.C., et al., (2003) Proliferation and neuronal differentiation of mitotically active cells following traumatic brain injury. Exp Neurol. **183**(2): p. 406-17.
11. Miller, S.P., et al., (2005) Patterns of brain injury in term neonatal encephalopathy. J Pediatr. **146**(4): p. 453-60.
12. Szele, F.G. and M.F. Chesselet, (1996) Cortical lesions induce an increase in cell number and PSA-NCAM expression in the subventricular zone of adult rats. J Comp Neurol. **368**(3): p. 439-54.
13. Chen, Z.G., et al., (2003) Effects of ganglioside GM1 on reduction of brain edema and amelioration of cerebral metabolism after traumatic brain injury. Chin J Traumatol. **6**(1): p. 23-7.
14. Acosta, S.A., et al., (2013) Long-term upregulation of inflammation and suppression of cell proliferation in the brain of adult rats exposed to traumatic brain injury using the controlled cortical impact model. PLoS One. **8**(1): p. e53376.
15. Lois, C., J.M. Garcia-Verdugo, and A. Alvarez-Buylla, (1996) Chain migration of neuronal precursors. Science. **271**(5251): p. 978-81.
16. Jankovski, A. and C. Sotelo, (1996) Subventricular zone-olfactory bulb migratory pathway in the adult mouse: cellular composition and specificity as determined by heterochronic and heterotopic transplantation. J Comp Neurol. **371**(3): p. 376-96.
17. Jin, K., et al., (2003) Directed migration of neuronal precursors into the ischemic cerebral cortex and striatum. Mol Cell Neurosci. **24**(1): p. 171-89.
18. Yang, Z., et al., (2007) Sustained neocortical neurogenesis after neonatal hypoxic/ischemic injury. Ann Neurol. **61**(3): p. 199-208.
19. Yang, Z. and S.W. Levison, (2007) Perinatal hypoxic/ischemic brain injury induces persistent production of striatal neurons from subventricular zone progenitors. Dev Neurosci. **29**(4-5): p. 331-40.
20. Buono, K.D., *Analyses of Mouse Neural Precursor Responses to Leukemia Inhibitor Factor and Hypoxia/Ischemia*, in *Graduate School of Biomedical Sciences*2011, University of Medicine and Dentistry of New Jersey: Newark. p. 1-200.

21. Rothstein, R.P. and S.W. Levison, (2002) Damage to the choroid plexus, ependyma and subependyma as a consequence of perinatal hypoxia/ischemia. Dev Neurosci. **24**(5): p. 426-36.
22. Romanko, M.J., R.P. Rothstein, and S.W. Levison, (2004) Neural stem cells in the subventricular zone are resilient to hypoxia/ischemia whereas progenitors are vulnerable. J Cereb Blood Flow Metab. **24**(7): p. 814-25.
23. Anderson, V., et al., (2000) Recovery of intellectual ability following traumatic brain injury in childhood: impact of injury severity and age at injury. Pediatr Neurosurg. **32**(6): p. 282-90.
24. Felling, R.J., et al., (2006) Neural stem/progenitor cells participate in the regenerative response to perinatal hypoxia/ischemia. J Neurosci. **26**(16): p. 4359-69.
25. Alagappan, D., et al., (2009) Brain injury expands the numbers of neural stem cells and progenitors in the SVZ by enhancing their responsiveness to EGF. ASN Neuro. **1**(2).
26. Covey, M.V., et al., (2010) Defining the critical period for neocortical neurogenesis after pediatric brain injury. Dev Neurosci. **32**(5-6): p. 488-98.
27. Demeurisse, G., (2000) Mechanisms of functional restoration after brain injury. Acta Neurol Belg. **100**(2): p. 77-83.
28. Richardson, R.M., D. Sun, and M.R. Bullock, (2007) Neurogenesis after traumatic brain injury. Neurosurg Clin N Am. **18**(1): p. 169-81, xi.
29. Aschermann, M., et al., (1987) [Comparison of left ventricular function in chronic postinfarction aneurysms in the anterior, lateral, apical and diaphragmatic location]. Cas Lek Cesk. **126**(40): p. 1238-41.
30. Kolb, E., (1987) [New knowledge of the structure and action of animal cell growth and hematopoiesis-regulating factors]. Z Gesamte Inn Med. **42**(20): p. 565-70.
31. Kolb, B., C. Holmes, and I.Q. Whishaw, (1987) Recovery from early cortical lesions in rats. III. Neonatal removal of posterior parietal cortex has greater behavioral and anatomical effects than similar removals in adulthood. Behav Brain Res. **26**(2-3): p. 119-37.
32. Brazel, C.Y., et al., (2004) Perinatal hypoxia/ischemia damages and depletes progenitors from the mouse subventricular zone. Dev Neurosci. **26**(2-4): p. 266-74.
33. Yang, Z. and S.W. Levison, (2006) Hypoxia/ischemia expands the regenerative capacity of progenitors in the perinatal subventricular zone. Neuroscience. **139**(2): p. 555-64.
34. Covey, M.V., et al., (2011) Opposite effect of inflammation on subventricular zone versus hippocampal precursors in brain injury. Ann Neurol.
35. Shen, C.C., et al., (2010) Characterization of endogenous neural progenitor cells after experimental ischemic stroke. Curr Neurovasc Res. **7**(1): p. 6-14.
36. Cheng, W.Y., et al., (2013) Luteolin inhibits migration of human glioblastoma U-87 MG and T98G cells through downregulation of Cdc42 expression and PI3K/AKT activity. Mol Biol Rep.
37. Yin, R.X., et al., (2006) [Nestin activation after rat cerebral ischemia-reperfusion injury and its changes in response to Tongxinluo treatment]. Nan Fang Yi Ke Da Xue Xue Bao. **26**(6): p. 777-9.
38. Zhang, R.L., et al., (2011) Ascl1 lineage cells contribute to ischemia-induced neurogenesis and oligodendrogenesis. J Cereb Blood Flow Metab. **31**(2): p. 614-25.
39. Sundholm-Peters, N.L., et al., (2005) Subventricular zone neuroblasts emigrate toward cortical lesions. J Neuropathol Exp Neurol. **64**(12): p. 1089-100.
40. Goings, G.E., V. Sahni, and F.G. Szele, (2004) Migration patterns of subventricular zone cells in adult mice change after cerebral cortex injury. Brain Res. **996**(2): p. 213-26.
41. Yang, Z., et al., (2007) Sustained neocortical neurogenesis after neonatal hypoxic/ischemic injury. Ann Neurol.
42. Yang, Z., Y. You, and S.W. Levison, (2008) Neonatal hypoxic/ischemic brain injury induces production of calretinin-expressing interneurons in the striatum. J Comp Neurol. **511**(1): p. 19-33.

43. Shi, J., et al., (2007) Injury-induced neurogenesis in Bax-deficient mice: evidence for regulation by voltage-gated potassium channels. The European journal of neuroscience. **25**(12): p. 3499-512.
44. Mattson, M.P., (2008) Glutamate and neurotrophic factors in neuronal plasticity and disease. Ann N Y Acad Sci. **1144**: p. 97-112.
45. Brazel, C.Y., et al., (2005) Glutamate enhances survival and proliferation of neural progenitors derived from the subventricular zone. Neuroscience. **131**(1): p. 55-65.
46. Bessis, A., et al., (2007) Microglial control of neuronal death and synaptic properties. Glia. **55**(3): p. 233-8.
47. Liberto, C.M., et al., (2004) Pro-regenerative properties of cytokine-activated astrocytes. J Neurochem. **89**(5): p. 1092-100.
48. Myer, D.J., et al., (2006) Essential protective roles of reactive astrocytes in traumatic brain injury. Brain.
49. Mignone, J.L., et al., (2004) Neural stem and progenitor cells in nestin-GFP transgenic mice. J Comp Neurol. **469**(3): p. 311-24.